Atomistic study of intrinsic defect migration in 3C-SiC

Fei Gao,[1,*] William J. Weber,[1] M. Posselt,[2] and V. Belko[3]
[1]*Fundamental Science Directorate, Pacific Northwest National Laboratory, P.O. Box 999, Richland, Washington 99352, USA*
[2]*Forschungszentrum Rossendorf, Institute of Ion Beam Physics and Materials Research, P.O. Box 510119, D-01314 Dresden, Germany*
[3]*Department of Mathematical Physics, Belarus State University, F. Skorina Avenue 4, 220050 Minsk, Belarus*
(Received 24 September 2003; revised manuscript received 16 December 2003; published 25 June 2004)

Atomic-scale computer simulations, both molecular dynamics (MD) and the nudged-elastic band methods, have been applied to investigate long-range migration of point defects in cubic SiC (3C-SiC) over the temperature range from $0.36T_m$ to $0.95T_m$ (melting temperature). The point defect diffusivities, activation energies, and defect correlation factors have been obtained. Stable C split interstitials can migrate via the first- or second-nearest-neighbor sites, but the relative probability for the latter mechanism is very low. Si interstitials migrate directly from one tetrahedral position to another neighboring equivalent position by a kick-in/kick-out process via a split-interstitial configuration. Both C and Si vacancies jump to one of their equivalent sites through a direct migration mechanism. The migration barriers obtained for C and Si interstitials are consistent with the activation energies observed experimentally for two distinct recovery stages in irradiated SiC. Also, energy barriers for C interstitial and vacancy diffusion are in reasonable agreement with *ab initio* data.

DOI: 10.1103/PhysRevB.69.245205 PACS number(s): 61.72.Ji, 66.30.Dn, 71.15.Pd, 61.72.Vv

I. INTRODUCTION

Due to its outstanding electrical, thermal, and mechanical properties, silicon carbide (SiC) has attracted extensive experimental and theoretical investigations because of its potential use in electronic and optoelectronic devices,[1,2] as well as nuclear applications.[3] The wide band gap of SiC makes possible the operation of solid-state devices for high-temperature or high current/power applications, and its chemical and mechanical stability under irradiation leads to applications as structural components for both fusion[4] and fission[5] reactors. In device processing, ion implantation is an important doping technique for SiC, since the low mobility of the most desirable dopants[6] excludes the application of dopant in-diffusion. On the other hand, ion implantation offers the advantage of precise control of dopant concentrations over well-defined depth distributions. However, irradiation inescapably results in the creation of defects and topological disorder, which not only inhibit electrical activation of the implanted dopants, but also deteriorate the properties of silicon carbide materials and devices for nuclear applications. Temperatures above 1800 K are required to electrically activate the dopants. While irradiation-induced defects can be annihilated by annealing, the defect kinetics during thermal annealing leads to the formation of dislocation loops due to the precipitation of interstitials.[7]

Knowledge of the defect migration and diffusion processes is crucial to understanding the response of SiC to ion implantation and thermal annealing processes, as well as to irradiation damage. Consequently, a number of experimental measurements have been carried out to study defect recovery in SiC following isochronal annealing[8–10] by channeling Rutherford backscattering spectrometry and positron lifetime spectroscopy and Doppler broadening.[11] However, it is difficult to determine the relative contributions of various defects and their clusters to these recovery stages. Atomic-level investigations of defect properties, defect migration, and diffusion, as well as diffusion mechanisms, using either *ab initio* methods or molecular dynamics with empirical potentials, have been demonstrated to be valuable techniques to interpret experimental observations. *Ab initio* calculations are quite accurate but require very intensive computational efforts. Molecular dynamics (MD) simulations based on empirical potentials are far less computationally demanding, and calculations have been carried out on large systems with time scales up to a few hundred nanoseconds. In this paper, MD simulations and the nudged-elastic band method[12] are employed to study defect migration and minimum-energy paths, and to characterize the mechanisms of defect diffusion in 3C-SiC.

II. COMPUTATIONAL METHOD

MD simulations of defect diffusion were performed in a cubic crystalline cell, with ⟨100⟩-axis orientation, that contains 8000 atoms with periodic boundary conditions and zero pressure.[13] The interactions between atoms were described using a Brenner type potential[14] that was developed based on various equilibrium properties, and the formation energies for stable defect configurations were determined by density-functional theory.[15] Defect diffusion was simulated in the temperature range from $0.36T_m$ to $0.95T_m$, where T_m is the melting temperature (2800 K). Additionally, the nudged-elastic-band method[12] was used to determine the minimum-energy paths and energy barriers for migration. In the MD simulations, the self-diffusion coefficient D can be determined from the summation of the squared displacements of all atoms N in the simulation cell

$$D = \frac{\sum_{i=1}^{N} [\vec{r}_i(t) - \vec{r}_i(0)]^2}{6t}, \tag{1}$$

which is accurate in the limit of large simulation time t. Therefore, the simulations were performed over several

nanoseconds. The quantity $\Sigma_{i=1}^{N}[\vec{r}_i(t)-\vec{r}_i(0)]^2$ was plotted as a function of time, and the self-diffusion coefficient was determined from the average slope.[16] Another possibility to calculate the defect diffusion coefficient is given by the following relationship:[17]

$$D = f_d \frac{\Delta^2 \Gamma}{6}, \tag{2}$$

where Δ and Γ are the defect jump length and jump frequency, respectively, and f_d is the defect correlation factor that can be calculated using the angle between the i^{th} and j^{th} jumps of the defect θ_{ij}.[17] The expression for f_d is

$$f_d = 1 + \frac{2}{n}\sum_{i=1}^{n-1}\sum_{j=i+1}^{n}\langle \cos\,\theta_{ij}\rangle, \tag{3}$$

where n is the total number of jumps. Equation (3) is accurate for large number of jumps. In the present MD simulations, the jump of a dumbbell interstitial is recorded when the dumbbell center of mass moves from one site to the first-nearest- or the second-nearest-neighbor site, which depends on the migration mechanisms (see below), while the jump length is an average value obtained by summarizing all possible jump distances and divided by the total number of jumps.

With self-diffusion coefficients obtained at different temperatures, the activation energy for defect migration E_m can be estimated from the Arrhenius relation

$$D = D_0 \exp\left(-\frac{E_m}{k_B T}\right), \tag{4}$$

where D_0 is the preexponential factor and k_B is the Boltzmann constant.

III. RESULTS AND DISCUSSIONS

For the diffusion of a C interstitial at $T=1500$ K, the quantity $\Sigma_{i=1}^{N}[\vec{r}_i(t)-\vec{r}_i(0)]^2$ and the number of jumps of a defect are shown in Fig. 1. In this case, the simulation started from the C-C⟨100⟩ dumbbell configuration, which is the most stable C interstitial configuration in 3C-SiC.[15,18] Although there exist some fluctuations in $\Sigma_{i=1}^{N}[\vec{r}_i(t)-\vec{r}_i(0)]^2$, all the dependences are approximately linear with time, and the self-diffusion coefficients can be calculated via Eq. (1) with reasonable accuracy. The slight decrease in the Si mean-square displacement (MSD) is due to the initial temperature scale that may cause the atoms to be largely displaced from their original positions, but the Si MSD is almost constant after 1.2 ns equilibration. It should be noted that the initial temperature scale may lead the C-C dumbbell interstitial to a high-energy configuration. Consequently, the MD block is equilibrated for 50 ps before recording the squared displacements of atoms and jumps, which guarantees that the local heat of the interstitial disperses into the surrounded material and the interstitial stays at the low-energy configuration. During the simulation, a large number of jumps are observed, as shown in Fig. 1, but most of the first-nearest-neighbor jumps, on average, do not cause the defect to be permanently displaced. The reason for this behavior is discussed later. The diffusion coefficients estimated for C and Si interstitials in SiC are given in Fig. 2 as a function of reciprocal temperature. The data follow an Arrhenius relationship [Eq. (4)], and the corresponding energies, preexponential factors, and defect correlation factors for C and Si interstitials are summarized in Table I.

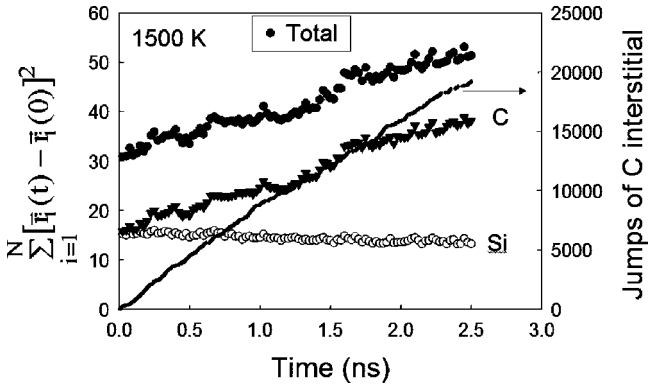

FIG. 1. Temporal evolution of the mean-square displacements (MSD's) of atoms ($\Sigma_{i=1}^{N}[\vec{r}_i(t)-\vec{r}_i(0)]^2$) and the number of jumps of a C interstitial at 1500 K in SiC. The contributions to the total MSD by Si (○) and C (▼) atoms are presented separately, where only the C interstitial contributes to the increase in the total (●) MSD. The decrease in the Si MSD is due to the initial temperature scale that may cause the atoms to be largely displaced from their original positions, but the Si MSD is almost constant after 1.2 ns equilibration.

The migration mechanisms for the self-interstitials have been identified by careful analysis of the computer-generated trajectories. For C interstitials, two migration pathways have been observed. The first is a nearest-neighbor jump via a Si site, and the second is a jump from a split configuration on a C site to another split configuration on a next-nearest-neighbor C site. Four snapshots of the nearest-neighbor jump mechanism at $T=1500$ K are shown in Fig. 3. The starting configuration is a C-C⟨100⟩ interstitial centered at a C site, as shown in Fig. 3(a), and this dumbbell is found to change its orientation. The movement of the dumbbell along the new

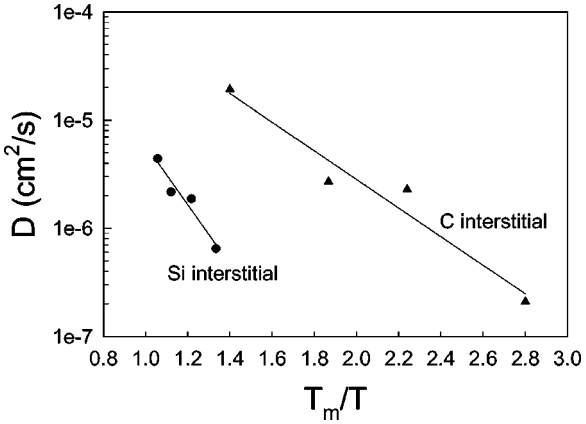

FIG. 2. Self-diffusion coefficients as a function of reciprocal temperature for C and Si interstitials in SiC, where the melting temperature T_m is 2800 K.

TABLE I. Migration energies E_m(eV), pre-exponential factors $D_0(10^{-3}\ \mathrm{cm}^2/\mathrm{s})$, and defect correlation factors f_d for interstitials in SiC, along with *ab initio* data.[19] Also included are related experimental values (eV). The migration energies for vacancy diffusion are the saddle-point energies obtained using the nudged-elastic-band method.

Defect	Simulation			*Ab initio*	Experiment
	E_m	D_0	f_d	E_m	Activation energy
C interstitial	0.74±0.05	1.23	0.27	0.5	0.89±0.02 (Ref. 10)
Si interstitial	1.53±0.02	3.30	0.86		1.5±0.3 (Ref. 9), 1.6 (Ref. 20)
C vacancy	4.10			3.5	
Si vacancy	2.35				

orientation leads to strong interactions of the C interstitial with one of the nearest Si atoms, thereby forming a C-Si dumbbell interstitial, as indicated in Fig. 3(b). It is found that the probability for the C interstitial to move back to the starting position is much higher than for it to jump to another C site, because this process apparently involves the rotation of the C-Si dumbbell, as seen in Figs. 3(c) and 3(d). The final configuration is shown in Fig. 3(d), forming a C-C dumbbell interstitial at the second-nearest-neighbor lattice site with respect to the starting position. As for the second-neighbor jump, the migration path is obviously simpler. The C-C dumbbell changes its orientation from initial ⟨100⟩ to ⟨110⟩ direction, and then moves along the ⟨110⟩ direction, causing the C interstitial to pass through a constriction consisting of two Si atoms. Further movement along an equivalent ⟨110⟩ direction results in the formation of a C-C dumbbell interstitial at the second-nearest-neighbor distance. However, the probability for the latter pathway to occur is much lower than that for the former migration mechanism, and only a few events are observed at high temperature, which may suggest that the energy barrier for the second-neighbor jump is higher than that for the first-neighbor jump via Si lattice sites. For a Si interstitial, only one migration mechanism is observed, which consists of a kick-in/kick-out process via a split-interstitial configuration. This mechanism is clearly demonstrated in Fig. 4, which shows three stages of the migration process. During the simulation, the Si interstitial spends most of its time staying in a tetrahedral position, namely $\mathrm{Si_{TC}}$, which is the most stable configuration among all possible Si interstitial configurations.[14,18] As soon as a Si-Si split interstitial is formed by the kick-in process, as shown in Fig. 4(b), one of the two Si atoms is immediately kicked out from the corresponding lattice site to a Si tetrahedral position. The forward jump leads to the migration of the Si interstitial, as indicated in Fig. 4(c). The transition process is fast, and takes only a few hundred MD time steps (about 0.01 ps).

The first migration mechanism found in the MD simulations for a C interstitial is generally consistent with a possible pathway suggested by the saddle-point calculations using an *ab initio* method.[19] This may suggest that the global picture derived from the present simulations of self-diffusion is qualitatively correct. Estimation of the defect correlation factor using Eq. (3) for C interstitials results in $f_d=0.27$, which indicates a large fraction of backward jumps of C atoms in the vicinity of Si sites. As described above, a C interstitial can jump to a Si site, forming a C-Si dumbbell interstitial. However, in order to jump forward, this dumbbell needs to change orientation, which decreases the probability for a forward jump. As a result, a large number of backward jumps occur, which is consistent with the low correlation factor obtained. The defect correlation factor for Si interstitials is estimated to be 0.86.

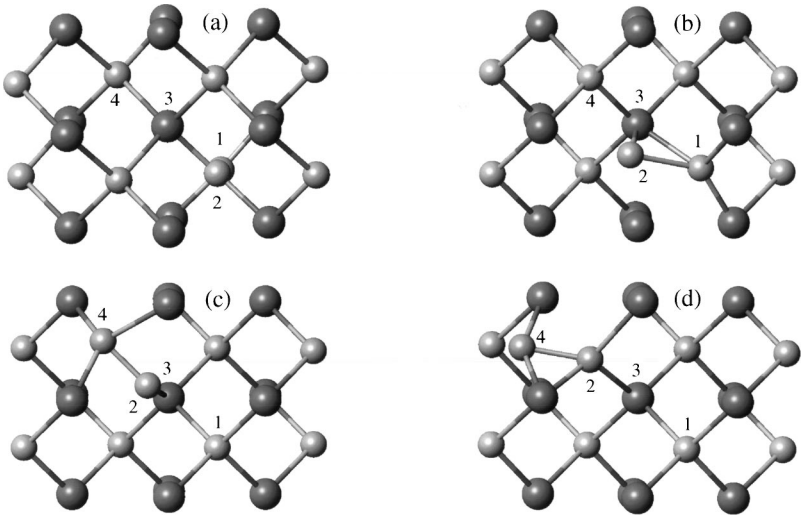

FIG. 3. Four snapshots showing the migration path for the first-neighbor jump mechanism of a C interstitial at $T=1500$ K, where the atoms involving the jump process are numbered. The light and dark spheres represent C and Si atoms, respectively. (a) Initial C-C⟨100⟩ dumbbell configuration at a C site, as indicated by atoms 1 and 2; (b) the formation of a C-Si dumbbell at a Si site; (c) the rotation of the C-Si dumbbell in order to jump forward; and (d) final C-C dumbbell configuration at the second nearest-neighbor distance away, as presented by atoms 2 and 4.

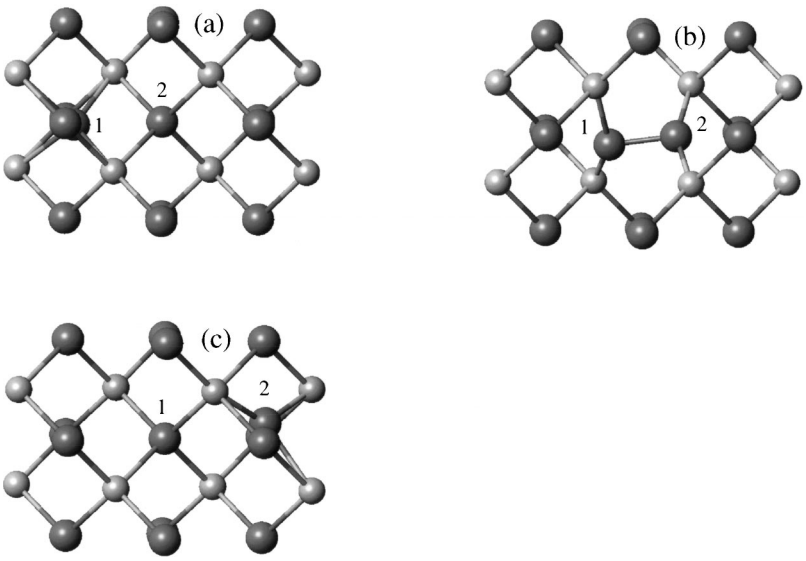

FIG. 4. Atomic plots showing three snapshots of migration path for a Si interstitial at $T = 2500$ K. (a) Initial tetrahedral position, (b) intermediate position forming a Si-Si split interstitial, and (c) final tetrahedral position at the second nearest-neighbor distance way.

Several attempts were carried out to simulate vacancy migration at high temperatures (close to the melting temperature), but only a few jumps were observed for a Si vacancy within simulation time (~8 ns), and no jumps occurred for a C vacancy. These simulations suggest that the migration energies for vacancies are very high. Nonetheless, the migration of the Si vacancy was found to occur by jumps of next-nearest-neighbor atoms to the vacancy site, and a similar pathway is assumed for a C vacancy. Consequently, the nudged-elastic-band method has been employed to investigate the energy barriers along the given pathways. The results for vacancies are provided in Fig. 5. There are multiple saddle points along the path for a Si vacancy, but only one saddle point occurs along the path for a C vacancy. The migration energies, which are included in Table I, are 2.35 and 4.10 eV for Si and C vacancies, respectively. The energy barriers calculated by the nudged-elastic-band method for C and Si interstitials are 0.81 and 1.51 eV, respectively, which are consistent with those obtained by MD simulations.

The migration energies for both interstitials and vacancies are summarized in Table I, together with experimental data from recovery processes in ion irradiated[9,10] and neutron damaged[20] SiC, as well as the *ab initio* results. It can be seen that the present MD results for the C interstitials and vacancies are in reasonable agreement with the *ab initio* calculations,[19] which are based on density-functional theory. Isochronal annealing of damage accumulation in ion-irradiated SiC has suggested that three distinct thermal recovery processes exist between 150 and 700 K.[9,10] The first thermal recovery process, which occurs below room temperature, has been experimentally estimated to have an activation energy of 0.3 ± 0.15,[9] and based on recent atomistic calculations,[21] this low-temperature recovery process is consistent with the recombination of close Frenkel pairs, which represent 60% of the interstitials that survive in a collision cascade. The thermal recovery process that occurs at about 450 K has been recently estimated to have an activation energy of about 0.9 ± 0.2,[22] which is consistent with the calculated migration energy for the C interstitial. Activation energy for the third thermal recovery process, which is observed at about 650 K, has been estimated to be 1.5 ± 0.3 eV in ion-irradiated SiC (Ref. 9) and 1.6 eV in neutron-irradiated SiC,[20] which is consistent with the calculated migration energy for Si interstitials. Thus, it may be

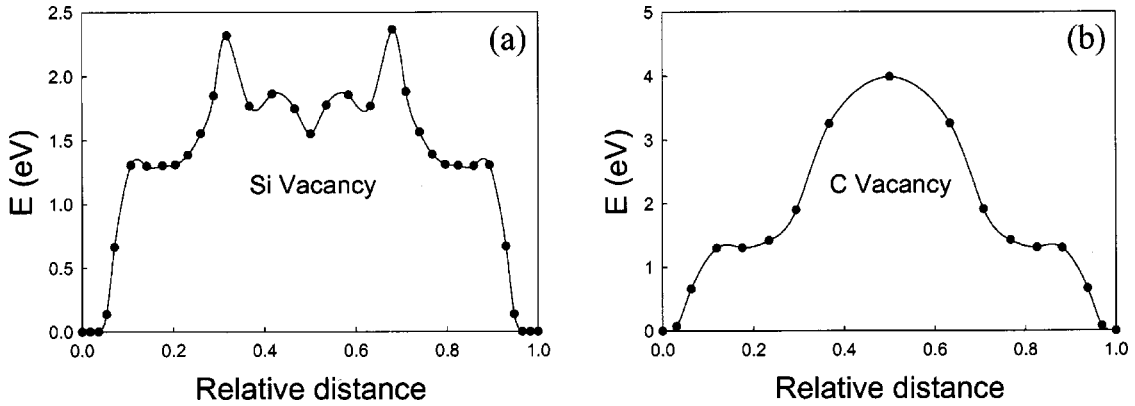

FIG. 5. Potential barriers obtained by the nudged-elastic band method along the given pathways for a Si vacancy (a) and a C vacancy (b).

assumed that the thermal recovery processes observed in irradiated SiC above room temperature are associated with the long-range migration of C and Si interstitials.

IV. SUMMARY

To summarize, molecular dynamics method has been employed to simulate long-range migration of point defects in 3C-SiC. C interstitials can migrate via the first-neighbor or second-neighbor sites, whereas Si interstitials jump directly from one tetrahedral position to an equivalent position by a kick-in/kick-out process via a Si-Si split-interstitial configuration. The migration energies are estimated to be 0.74 and 1.53 eV for C and Si interstitials, respectively. These results are consistent with experimentally determined activation energies for thermal recovery processes at about 450 and 650 K. This suggests that these processes are associated with the long-range migration of C and Si interstitials, respectively. The small defect correlation factor for C interstitials (f_d=0.27) indicates that a large number of backward jumps occur, which is consistent with the defect geometries in SiC. Both Si and C vacancies jump to one of their equivalent sites through a direct migration mechanism. The nudged-elastic-band method has also been used to study the energy barriers along pathways corresponding to the diffusion mechanisms that were observed in the MD simulations. The activation energies for vacancy migration are 2.35 and 4.10 for Si and C, respectively. By considering the migration mechanisms of C interstitials and vacancies explored by *ab initio* method and available experimental data, respectively, the present simulations provide a very consistent understanding of defect diffusion processes in SiC.

ACKNOWLEDGMENT

This research was supported by the Division of Materials Sciences and Engineering, Office of Basic Energy Sciences, U.S. Department of Energy under Contract No. DE-AC06-76RLO 1830.

*Corresponding author. FAX: 1–509 376 5016. Email address: fei.gao@pnl.gov

[1] W. J. Choyke and G. Pensl, MRS Bull. **22**, 25 (1997).
[2] W. Bolse, Nucl. Instrum. Methods Phys. Res. B **148**, 83 (1999).
[3] B. G. Kim, Y. Choi, J. W. Lee, D. S. Sohn, and G. M. Kim, J. Nucl. Mater. **281**, 163 (2000).
[4] L. Giancarli, J. P. Bonal, A. Caso, G. Le Marois, N. B. Morley, and J. F. Salavy, Fusion Eng. Des. **41**, 165 (1998).
[5] J. A. Lake, R. G. Bennett, and J. F. Kotek, Sci. Am. **286** [1], 73 (2002).
[6] V. Khemka, P. Patel, N. Ramungul, T. P. Chow, M. Ghesso, and J. Kretchmer, J. Electron. Mater. **28**, 167 (1999).
[7] P. O. Å. Persson, L. Hultman, M. S. Janson, A. Hallén, J. D. Persio, and R. Martinez, Appl. Phys. Lett. **76**, 2725 (2000).
[8] J. Chen, P. Jung, and H. Klein, J. Nucl. Mater. **258-263**, 1803 (1998).
[9] W. J. Weber, W. Jiang, and S. Thevuthasan, Nucl. Instrum. Methods Phys. Res. B **175-177**, 26 (2001).
[10] Y. Zhang, W. J. Weber, W. Jiang, A. Hallén, and G. Possnert, J. Appl. Phys. **91**, 6388 (2002).
[11] W. Puff, A. G. Balogh, and P. Mascher, Mater. Res. Soc. Symp. Proc. **540**, 177 (1999).
[12] M. R. Sorensen, K. W. Jacobsen, and H. Jónsson, Phys. Rev. Lett. **77**, 5067 (1996).
[13] Yu. N. Osetsky, A. G. Mikhin, and A. Serra, Philos. Mag. A **72**, 361 (1995).
[14] D. W. Brenner, Phys. Rev. B **42**, 9458 (1990).
[15] F. Gao and W. J. Weber, Nucl. Instrum. Methods Phys. Res. B **191**, 504 (2002).
[16] G. H. Gilmer, T. Diaz de la Rubia, D. M. Stock, and M. Jaraiz, Nucl. Instrum. Methods Phys. Res. B **102**, 247 (1995).
[17] L. A. Girifalco, *Statistical Physics of Materials* (Wiley, New York, 1973), p. 257.
[18] F. Gao, E. J. Bylaska, W. J. Weber, and L. R. Corrales, Phys. Rev. B **64**, 245208 (2001).
[19] M. Bockstedte, M. Heid, A. Mattausch, and O. Pankratov, Mater. Sci. Forum **433-436**, 471 (2003).
[20] W. Primak, L. H. Fuchs, and P. P. Day, Phys. Rev. **103**, 1184 (1956).
[21] F. Gao and W. J. Weber, J. Appl. Phys. **94**, 4348 (2003).
[22] Y. Zhang, W. J. Weber, W. Jiang, C. M. Wang, A. Hallén, and G. Possnert, J. Appl. Phys. **93**, 1954 (2003).